Remote Sensing of Environment 112 (2008) 4120–4130

Contents lists available at ScienceDirect

Remote Sensing of Environment

journal homepage: www.elsevier.com/locate/rse

Assessment of C-band synthetic aperture radar data for mapping and monitoring Coastal Plain forested wetlands in the Mid-Atlantic Region, U.S.A.

Megan W. Lang [a,*], Eric S. Kasischke [b], Stephen D. Prince [b], Kyle W. Pittman [c]

[a] USDA—Agricultural Research Service, Hydrology and Remote Sensing Lab, 10300 Baltimore Avenue, Beltsville, Maryland, United States
[b] Department of Geography, University of Maryland, United States
[c] Geographic Information Science Center of Excellence, South Dakota State University, United States

ARTICLE INFO

Article history:
Received 12 March 2007
Received in revised form 27 July 2007
Accepted 11 August 2007

Keywords:
SAR
ENVISAT ASAR
ERS
Wetlands, Swamp
Forest
Hydroperiod
Hydrology
Ecosystem management

ABSTRACT

Multi-temporal C-band SAR data (C-HH and C-VV), collected by ERS-2 and ENVISAT satellite systems, are compared with field observations of hydrology (i.e., inundation and soil moisture) and National Wetland Inventory maps (U.S. Fish and Wildlife Service) of a large forested wetland complex adjacent to the Patuxent and Middle Patuxent Rivers, tributaries of the Chesapeake Bay. Multi-temporal C-band SAR data were shown to be capable of mapping forested wetlands and monitoring hydroperiod (i.e., temporal fluctuations in inundation and soil moisture) at the study site, and the discrimination of wetland from upland was improved with 10 m digital elevation data. Principal component analysis was used to summarize the multi-temporal SAR data sets and to isolate the dominant temporal trend in inundation and soil moisture (i.e., relative hydroperiod). Significant positive, linear correlations were found between the first principal component and percent area flooded and soil moisture. The correlation (r^2) between the first principal component (PC1) of multi-temporal C-HH SAR data and average soil moisture was 0.88 (p=<.0001) during the leaf-off season and 0.87 (p=<.0001) during the leaf-on season, while the correlation between PC1 and average percent area inundated was 0.82 (p=<.0001) and 0.47 (p=.0016) during the leaf-off and leaf-on seasons, respectively. When compared to field data, the SAR forested wetland maps identified areas that were flooded for 25% of the time with 63–96% agreement and areas flooded for 5% of the time with 44–89% agreement, depending on polarization and time of year. The results are encouraging and justify further studies to attempt to quantify the relative SAR-derived hydroperiod classes in terms of physical variables and also to test the application of SAR data to more diverse landscapes at a broader scale. The present evidence suggests that the SAR data will significantly improve routine wooded wetland mapping.

Published by Elsevier Inc.

1. Introduction

The biologic, aesthetic, and economic values of wetlands are now known to be disproportionately large compared to the often small percentage of the landscape they occupy. Wetlands in the Chesapeake Bay Watershed are especially vital as they help maintain water quality in one of the Nation's most productive estuaries (Chesapeake Bay Program, 1998; Tiner, 1987). Because of the high density of wetlands in the Mid-Atlantic Coastal Plain and development resulting from rapid population increase, this region is at high risk for future wetland loss. Forested wetlands, the most common type of wetland in the Chesapeake Bay Watershed, are especially at risk (U.S. Fish and Wildlife Service, 2002).

Wetland hydroperiod, or temporal variations in inundation and soil moisture, is the single most important factor in the formation and functioning of a wetland. Hydroperiod may result from complex and often small topographic variations in floodplain geomorphology, the type of soils present, and transfers of water into and out of the ecosystem. Small changes in water regime can cause large changes in wetland functioning, such as the potential of wetlands to transform and reduce nutrients (i.e., N and P) in ground and surface waters (Hamilton et al., 2007; Hattermann et al., 2006; Mitsch & Gosselink, 2000). These nutrients are responsible for water quality reductions in the Chesapeake Bay and have been the focus of numerous research studies and a high level of public and governmental concern (Boesch et al., 2001).

Although nutrient dynamics in the Chesapeake Bay itself have been rigorously studied, the fate and transport of nutrients in the Chesapeake Bay Watershed have not been given as much attention (Boesch et al., 2001). Presently, the Chesapeake Bay Program and other management agencies are working to estimate pollution reduction rates attributable to wetlands (J. Okay, personal communication,). However, accurate and timely information on wetland extent and hydroperiod is needed to fully integrate these estimates into decision support tools. Anticipated changes to the Mid-Atlantic climate (Mid-Atlantic Regional Assessment Team, 2000) could alter the

* Corresponding author. Tel.: +1 301 504 5138; fax: +301 504 8931.
E-mail address: Megan.Lang@gmail.com (M.W. Lang).

0034-4257/$ – see front matter. Published by Elsevier Inc.
doi:10.1016/j.rse.2007.08.026

water balance in this region's wetlands (Moore et al., 1997), further emphasizing the need for a means of continuously monitoring forested wetland hydrology.

Federal and State governments have sponsored wetland mapping programs, but many of the resultant maps are out of date, especially in areas, such as the Mid-Atlantic, that are undergoing rapid development. In addition, these maps are static and do not represent the dynamic nature of wetland hydrology. Field monitoring of forested wetlands is costly at the broad scales required for ecosystem management and regulation. While aerial photography is used to map forested wetlands, this method is often limited by cloud cover and the need to photograph forested wetlands during the leaf-off period. Furthermore, aerial photograph acquisition and necessary human interpretation are time-consuming, somewhat subjective, and expensive (Lunetta & Balogh, 1999; Tiner, 1999), especially since many forested wetlands are difficult to identify in aerial photographs (Sader et al., 1995; Tiner, 1990).

Synthetic aperture radar (SAR) imaging systems have the capability to detect key hydrologic characteristics of wetlands: namely, the spatial and temporal patterns of inundation and soil moisture. The Wetlands Subcommittee of the Federal Geographic Data Committee (1992) found that the difficulty of acquiring cloud-free imagery during the optimal time period was a key obstacle to mapping wetlands with optical satellite data. However, SARs can collect imagery regardless of solar radiation and cloud cover because these systems provide their own energy for surface illumination at wavelengths that penetrate clouds (Hess et al., 1995; Kasischke et al., 2003; Morrissey et al., 1994; Townsend, 2002; Townsend & Walsh, 1998; Wang et al., 1995). For this reason, SAR data can be used to produce wetland maps during optimal time periods and with greater frequency than optical images. Another advantage is that radar data can be processed semi-automatically using image processing software and batch programming and do not require the same level of expertise needed for aerial photograph interpretation, which is often done by hand. In contrast, aerial photographs are better suited for distinguishing different types of vegetation and for the mapping of herbaceous wetlands (i.e., marshes).

Although previous studies (Townsend, 2000; Townsend & Walsh, 1998) have demonstrated that C-band SAR data (wavelengths of ~6 cm) can detect relatively large areas of inundation beneath the forest canopy, these data have not been used to map less extensive flooding beneath forest canopies in the smaller floodplains that are more typical of the Chesapeake Bay Watershed. Nor have these data been compared to detailed field measurements of inundation and soil moisture. Little is known about the ability of C-band SAR data to distinguish different amounts of inundation (i.e., percent area inundated) and levels of soil moisture below the forest canopy that are indicative of hydroperiod.

The goal of this research study was to investigate the utility of C-band SAR data in mapping forested wetlands and monitoring forested wetland hydroperiod in the Mid-Atlantic U.S., and whether optical data can be used to enhance classification accuracy. This study provides a general approach to forested wetland mapping that builds upon documented relationships between inundation and SAR data response (Townsend, 2002; Townsend & Walsh, 1998) and moves towards an operational wetland hydrology monitoring solution. The contribution of Landsat Enhanced Thematic Mapper imagery to the forested wetland mapping process was determined. Maps created with multi-temporal ERS-1/2 (i.e., AMI — Advanced Microwave Instrument) and ENVISAT Advanced Synthetic Aperture Radar (ASAR) data were compared with direct observations of hydrology (i.e., inundation and soil moisture) and U.S. Fish and Wildlife Service (FWS) National Wetland Inventory maps. The utility of incorporating digital elevation data into the wetland mapping process was also explored. This mapping exercise was primarily conducted over a wildlife preserve near Laurel, Maryland, located on the upper Coastal Plain of the Mid-Atlantic, U.S. This analysis constitutes a necessary step towards improved forested wetland monitoring and provides ecologists and managers with vital information that is often missing or inferred using less direct means.

2. Background

2.1. Conventional mapping of forested wetlands

Since the 1970's, wetlands have been mapped using combinations of optical imagery and field data. In the U.S. the majority of wetland maps are produced by government agencies, such as the FWS, National Oceanic and Atmospheric Administration (NOAA), and Environmental Protection Agency (EPA). The most comprehensive national mapping effort was undertaken through the FWS's National Wetlands Inventory (NWI). The NWI produces wetland maps using interpretation of mid- to high altitude aerial photographs combined with field verification and collateral data (Federal Geographic Data Committee, 1992). The NWI maps usually err less by commission and more by omission; thus, if a wetland is indicated on a NWI map, there is a high probability that one exists or did at the time the photograph was taken (Nichols, 1994; Stolt & Baker, 1995). Forested wetlands are one of the most difficult types of wetlands to map using NWI's aerial photograph approach (Tiner, 1990). Estimates of the extent of NWI's forested wetland omission errors vary widely (Kudray & Gale, 2000; Rolband, 1995). The majority of NWI maps for the Mid-Atlantic Coastal Plain were generated using aerial photographs that are at least 20 years old. These maps are frequently out of date in areas undergoing rapid changes in wetland extent, such as that caused by beaver activity, forestry, drainage for agriculture, and various forms of construction. However, regardless of NWI's imperfections, NWI maps are one of the most commonly relied upon sources of wetland information in the U.S. and have been used to support management and regulatory decisions (Kudray & Gale, 2000).

Due to the high costs in time and money required to map wetlands with aerial photography, newer techniques are being developed by the FWS and others to update wetland maps (U.S. Fish and Wildlife Service, 2002), including utilization of satellite data. The advantages of using satellite data for wetland mapping include timeliness and cost savings, along with an inherently digital format that facilitates integration with other types of geospatial data and analyses using a geographic information system (Dobson et al., 1995; Federal Geographic Data Committee, 1992; Li & Chen, 2005). Unfortunately, visible and near-infrared satellite data alone have generally not produced adequate results without additional aerial photography and ground data, particularly for forested wetlands (Federal Geographic Data Committee, 1992; Li & Chen, 2005; Sader et al., 1995; Tiner, 1990). Although mid-infrared satellite data provide some increased sensitivity to spatial variations in hydrology (National Research Council, 1995), these data still do not provide the sensitivity to soil moisture (Neusch & Sties, 1999) or relatively small areas of inundation necessary to distinguish forested uplands from forested wetlands and to map hydroperiod. While Landsat Thematic Mapper data are usually not used alone to map forested wetlands, they have proved suitable for updating wetland maps. For example, techniques known as cross-correlation analysis (CCA) use multi-spectral satellite data to detect changes in land cover that have occurred since the wetland map was produced (Koeln & Bissonnette, 1999). However, CCA and other similar methods are limited to detecting changes within existing mapped wetland polygons. Therefore, these techniques are dependent on the existence of an accurate baseline map with low omission errors and cannot be used to detect newly formed wetlands.

2.2. Mapping forested wetlands using C-band SAR data

The scattering and reflection of microwave energy is sensitive to variations in soil moisture and the presence/absence of surface water, primarily due to the high dielectric constant of water. Microwave

energy from SAR sensors is usually measured as radar backscatter. The energy, as a fraction of incident energy from the sensor, is described as the backscatter coefficient (σ°) once it is normalized by pixel area. This energy is only partially attenuated by vegetation canopies (i.e., leaves and branches; Townsend, 2002; Townsend & Walsh, 1998), which permits the monitoring of inundation and soil moisture below the forest canopy. The presence/absence of leaves can have a significant effect on the attenuation of microwave energy as it passes through the forest canopy. Because greater canopy closure can decrease the amount of microwave energy which penetrates the forest canopy, the ability of SAR data to detect hydrology (i.e., inundation and soil moisture) below the forest canopy is greatest during the leaf-off season. The microwave energy that is transmitted through the canopy can then interact at the Earth's surface. Surface inundation (i.e., flooding) greatly increases radar backscatter from forests due to "double-bounce" backscatter, which occurs when energy emitted from the sensor bounces off the water surface away from the sensor and then off a tree trunk back towards the sensor (Richards et al., 1987). In the absence of inundation, increases in soil moisture are known to enhance radar backscatter (Kasischke et al., 2003; Wang et al., 1995). More detailed explanations of microwave scattering from forests are found in Dobson et al. (1995) and Wang et al. (1995).

The wavelength and polarization of microwave energy can influence the amount of energy that is reflected and scattered from the surface, and thus returned to the sensor. Energy transmitted from the SAR sensor towards the surface of the Earth is composed of an electric and a magnetic component. These two components travel orthogonal to one another and the orientation (e.g., vertical or horizontal) of the electric component of electromagnetic energy (perpendicular to the direction of travel) determines the polarization of that energy. Microwave energy that is both vertically transmitted and received (VV) does not pass as readily through forests as horizontally transmitted and received (HH) microwave energy (Hess et al., 1995; Wang et al., 1995). This is because the vertically polarized energy interacts more with large vertical structures (i.e., tree trunks) resulting in increased scattering and attenuation before the energy reaches the ground. For this reason, C-HH data are expected to be superior for the detection of inundation and soil moisture below the forest canopy. It is important to understand the varying limitations of VV and HH polarized data because the archives containing these polarizations differ in duration and availability (see below). Longer wavelength (L; ~20 cm) microwave energy is better suited for detecting forested wetlands (Costa 2004; Hess et al., 1990; Hess et al., 1995; Li & Chen 2005; Townsend 2002; Wang et al., 1995) than shorter wavelength microwave energy (C; ~6 cm) because it is better able to penetrate the forest canopy. However, no spaceborne L-HH sensors were collecting imagery at the time of this study. The duration of the L-HH imagery archive is also short. Three spaceborne, C-band SAR sensors were collecting imagery at the time of this study: ENVISAT ASAR (C-HH, C-VV, C-HV, and C-VH), RADARSAT-1 (C-HH), and ERS-2 (C-VV). While C-HH band SAR data are less suited for forested wetland studies than L-HH SAR data, C-HH SAR data have been used to monitor inundation patterns in some forested wetlands (Townsend, 2002). C-VV data from the ERS SARs have primarily been used to study herbaceous vegetation, but have also been successful in detecting inundation under forest canopies during the leaf-off period (Kasischke et al., 1997; Townsend, 2002). The combination of ERS-1 (launched in 1991), ERS-2 (launched in 1995), and ENVISAT (launched in 2002) provide over 15 years of continuous C-VV coverage while RADARSAT-1 (launched in 1995) and ENVISAT provide over ten years of historic C-HH data. While these satellites do not automatically collect data over the entire globe, there is an ample supply of historic C-band data for the Mid-Atlantic U.S. Coastal Plain. These sensors continue to collect data and archival scenes can be ordered from the European Space Agency (ESA), the Canadian Space Agency, the Alaska Satellite Facility, and various commercial data providers.

3. Methods

Wetland maps produced from combinations of Landsat Enhanced Thematic Mapper Plus (ETM+), ERS-2 (C-VV), and ENVISAT ASAR (C-HH and C-VV) data were compared to hydrologic data collected at the study site (i.e., percent area inundated and soil moisture; see Section

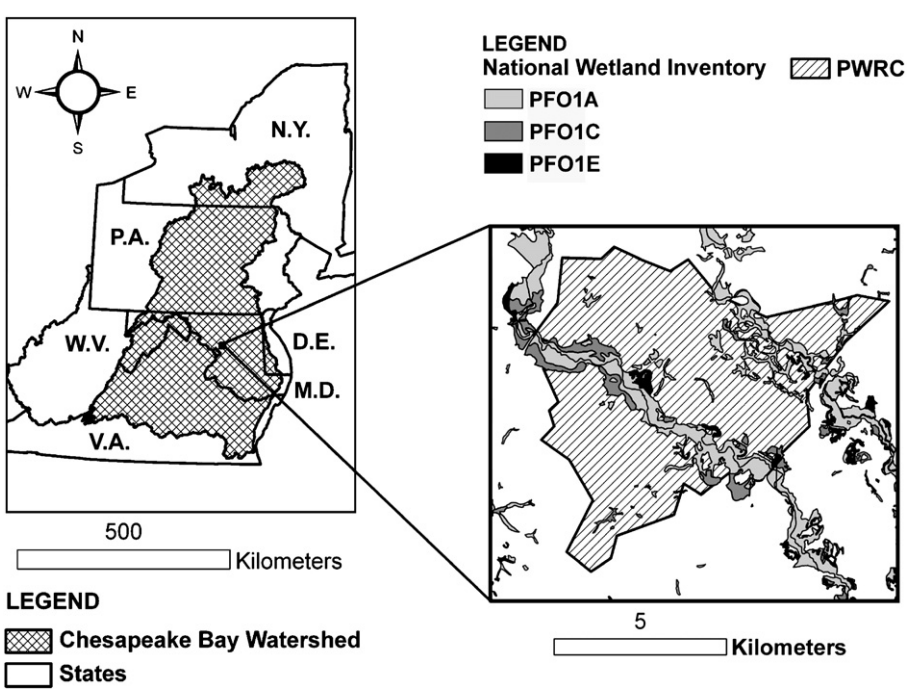

Fig. 1. Map of study area and forested wetlands as depicted by NWI. The three NWI categories include palustrine, broad-leaved deciduous forest with either seasonally flooded/saturated (PFO1E — longest flooding duration), seasonally flooded (PFO1C — longer flooding duration), or temporarily flooded (PFO1A — shorter flooding duration) wetlands. The aerial photograph used to create the NWI map was collected in the early 1980s.

3.2) and NWI wetland maps. Forest stand characteristics (i.e., percent canopy cover, relative tree basal area, and height of canopy trees) were measured to determine the potential for applying the methods developed through this study to other regions. It was hypothesized that certain types of C-band SAR data, namely C-HH data, would be better suited for detecting variations in hydrology (i.e., inundation and soil moisture) below the forest canopy and that the ability of all types of C-band SAR data to detect variations in hydrology would be greatest during the leaf-off season. Superior detection of hydrology by the different data sets was primarily tested by comparison of resultant maps and map components (PC1) with hydrologic data. Maps were compared with NWI to gauge the difference between the radar derived maps and standard wetland maps produced using optical imagery.

3.1. Study area

The study area is located in the Coastal Plain Physiographic Province between the cities of Washington, D.C. and Baltimore, Maryland, U.S.A (Fig. 1). The research was conducted in the Patuxent Wildlife Research Center (PWRC), the U.S. Department of Agriculture's Beltsville Agricultural Research Center, and Fort Meade. This study focused on upland and wetland areas surrounding the Patuxent and Middle Patuxent Rivers, both tributaries of the Chesapeake Bay.

The Patuxent River has a well-developed floodplain with numerous wetlands. Additional wetlands occur outside the floodplain in depressions and other topographic settings that result in accumulation of water. The braided channels of the Patuxent River are surrounded by levees that gradually decrease in elevation into backwater areas towards uplands on either side of the floodplain. Much of the floodplain is inundated for only part of the year, although the backwater areas can remain flooded for a much longer period of time. The timing of inundation and fluctuations in soil moisture (i.e., hydroperiod) at the study site are controlled by variations in evapotranspiration, precipitation, and the amount of water released from upstream dams.

3.2. Field observations

Measurements of percent area inundated, soil moisture, tree basal area, and percent tree canopy closure were made in twenty-four, 4 ha plots distributed through the study area (Fig. 2). Eight plots each were located in upland forests, wetland forests (usually backwater areas), and forests of intermediate hydrology. Intermediate plots were located in forests with hydroperiods that were wetter than upland sites and drier than wetland sites, and were usually found on or adjacent to levees surrounding the stream. Using aerial photographs, FWS NWI maps, and field reconnaissance, the plots were located in areas of relatively homogeneous forest type, forest cover, and hydrology. Plot corner locations were measured using a differentially-corrected global positioning system (GPS) and entered into a geographic information system (GIS) to extract the satellite data for each plot.

Hydrologic data (i.e., inundation and soil moisture) were collected approximately once per month during summer 2003 through summer 2004. For the collection of percent area inundated, the 4 ha plots were divided into 64 equal sub-sections of 25×25 m and percent area inundated was visually estimated in each sub-section using the Daubenmire cover class approach (where 1=1–5% inundation, 2=6–15%, 3=16–25%, 4=26–50%, 5=51–75%, 6=76–95%, and 7=96–100%; Daubenmire, 1968). The Daubenmire approach provides a relatively quick and inexpensive way to monitor area inundated when aerial surveying is impractical, as it was in this study. This method standardizes measurements collected by different individuals over extended periods of time (Korb et al., 2003). However, uncertainty was reduced in this study by limiting the collection of inundation data to one individual. For comparison to the satellite data, average inundation was calculated for 1 ha sub-plots (4 per plot). Volumetric soil water content was measured at eight locations distributed evenly within each plot using a time-domain reflectometer (Hydrosense ® meter, Campbell Scientific, Inc.). Five soil moisture measurements were taken at each location, one at the center and one at a random distance (1–10 m) in the four cardinal directions. These 40 measurements were then averaged for comparison with the SAR data.

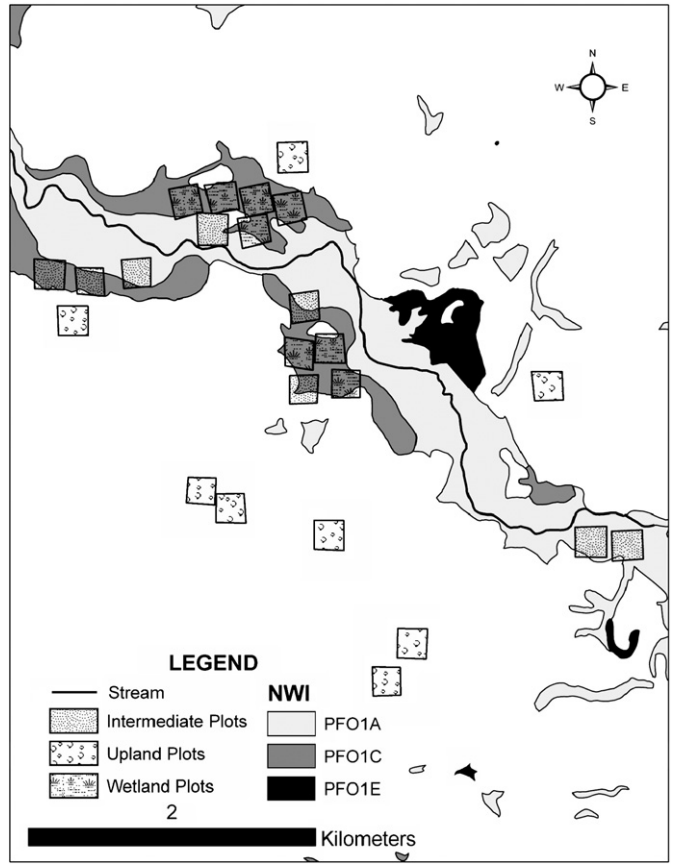

Fig. 2. Distribution of wetland, intermediate, and upland ground data collection plots relative to wetlands as depicted by NWI (see Fig. 1 for a description of wetland classes).

Relative basal area of canopy trees (i.e., the trees that compose the forest canopy) was collected from the 24 plots using a 2 m prism and the Bitterlich method (Shiver & Borders, 1996). Basal area was observed in nine areas, spread evenly throughout each plot and averaged for the entire plot. Percent canopy cover was measured at multiple times throughout the year (more frequently during the spring and fall) using digital hemispherical photos of the canopy. These measurements were collected at two wetland, two intermediate, and two upland sites. Photographs were taken at eight locations, spread evenly throughout each plot. Photos were standardized by tripod height and orientation, and analyzed with HemiView software (Vieglais & Rich, 1997).

3.3. Remote sensing data and analyses

The utility of various sources and polarizations of C-band SAR data was tested under both leaf-on and leaf-off conditions (Table 1), assessing the relative merits of C-HH SAR data and C-VV SAR data for mapping flooded forests throughout the year. The contribution of Landsat ETM+ to classification accuracy was also gauged. ERS (C-VV; 30 m) and ENVISAT ASAR (C-HH and C-VV; 30 m) images collected at an average incidence angle of ~23° were obtained from ESA. The ASAR

Table 1
Summary of spaceborne SAR data used to map forested wetlands

SAR data	Acquisition dates	Lf-off	Lf-on	C-HH	C-VV
C-HH ASAR	10/2/03, 10/28/03, 11/6/03, 12/2/03, 3/25/04, 4/20/04, & 4/29/04	X	X	X	
C-VV ASAR	10/2/03, 10/28/03, 11/6/03, 12/2/03, 3/25/04, 4/20/04, & 4/29/04	X	X		X
Leaf-Off ASAR	11/6/03, 12/2/03, 3/25/03, 4/20/04	X		X	
Leaf-On ASAR	7/15/03, 8/19/03, 10/2/03, 4/29/04, 5/25/04, & 6/3/04		X	X	
ERS	2/20/97, 3/22/95, 3/27/97, 3/28/98, & 11/27/97	X			X

Data type is indicated with an "X".

images were collected approximately once per month between July 2003 and June 2004. The ERS images were collected between 1995 and 1998 and selected based on conditions at the time the scene was collected, considering only data acquired when the deciduous trees were leafless, on rain-free days with above freezing temperatures.

The ERS precision images (PRI) initially calibrated by ESA were further calibrated and coregistered (BEST software, European Space Agency and Telespazio, 2007). The resultant data were georeferenced to UTM coordinates using a second-order polynomial transformation with nearest-neighbor resampling. The ASAR data were also delivered in PRI format but were geocoded by ESA. The georegisteration was later modified in the image headers to ensure spatial agreement among the data. The SAR intensity values were converted to dB (Rosich & Meadows, 2004). A combination of median and enhanced lee filters with kernel sizes of 3 and 5 pixels were used to reduce speckle and smooth areas of the image with similar ground cover. The use of small kernel sizes helped preserve edges. Pixel size, originally 12.5 m, was resampled to 30 m and a mask based on the Mid-Atlantic Regional Earth Science Applications Center (RESAC) tree canopy cover map (Goetz et al., 2000; comparable to widely available National Land Cover Dataset tree canopy maps) was applied to remove all areas with less than 45% tree canopy cover.

Multi-spectral Landsat ETM+ data from March 2000 were pre-processed by the Mid-Atlantic RESAC (Goetz et al., 2000). The RESAC pre-processing included orthorectification, radiometric calibration, conversion to exoatmospheric reflectance, and removal of clouds, cloud shadows, and topographic effects (Varlyguin et al., 2001). Six visible, near-infrared, and mid-infrared bands (30 m spatial resolution) and six tasseled cap (Kauth & Thomas, 1976) transforms, created using the original 6 bands, were used in combination with multi-temporal ENVISAT ASAR data and a USGS 1/3 arc sec DEM (~10 m horizontal resolution resampled to 30 m; U.S. Geological Survey, 2004) in a decision tree analysis (See5 software, Rulequest Research, 2004). The See5 software was linked with Erdas Imagine (Leica Geosystems) to intake the decision tree output and produce a raster classification. The decision tree/image processing software combination not only has the ability to produce a classification map, but it can also be used to identify the inputs which were used to create the map. The decision tree did not find the multi-spectral or the transformed (tasseled cap) bands to be useful in improving the discrimination of upland forest from wetland forest. Therefore, these data were eliminated from further study.

Multi-temporal SAR data were then used to create maps of forested wetlands as well as a map of forested wetland hydroperiod. A principal components analysis (PCA) of the multi-temporal SAR data (Bourgeau-Chavez et al., 2005) was used to further reduce image speckle and isolate sources of temporal variation between SAR images. PCA reduces temporal autocorrelation and presents information from multiple scenes in one or more principal components, the first containing the dominant temporal trend. Due to the high sensitivity of microwave energy to the presence of surface water, the first principal component (PC1) represented variations in image intensity associated with differences in hydrology. This was confirmed by expert knowledge of the study site gained from extensive field work and comparison of PC1 with hydrology and vegetation data collected at the 24 study plots. PC1 explained most of the variation found in the multi-temporal data (~95% for all multi-temporal ASAR groups and 87% for the multi-temporal ERS group).

PC1 was used to create two types of maps, a binary map (forested wetland and other) using a threshold value of PC1 and a multi-class forested wetland hydroperiod map using several thresholds of the PC1 values. To create the binary maps, the first principal component, the USGS DEM, and the forest mask were analyzed using a decision tree (Environment for Visualizing Images [ENVI], Research Systems, Inc.). Pixels were classified as wetland if they were in forested areas, on slopes of less than 15°, and if their backscatter coefficient exceeded a threshold (the backscatter boundary value) determined by inspection of the SAR and field data. Although the majority of wetlands are found on slopes of less than 8° (Sader et al., 1995), the 15 degree slope criteria was used due to study site wetlands on steeper slopes, often located at the base of floodplain terraces. Binary classifications were generated using C-HH ASAR data, C-VV ASAR data, leaf-on C-HH ASAR data, leaf-off C-HH ASAR data, and leaf-off C-VV ERS data (Table 1). The leaf-on/leaf-off distinction was made using field measurements of percent canopy closure, with visible sky fractions of >30% defined as leaf-off conditions and measurements <15% indicating leaf-on. Although visible sky fractions between 15% and 30% did occur, the collection of images during this time was minimal and these images were excluded from the leaf-off and leaf-on categories. Backscatter boundary values distinguishing upland forest from wetland forest were selected as −5 dB, −5 dB, −7 dB, −3.5 dB, and −5 dB for the C-HH ASAR (leaf-off and leaf-on), C-VV ASAR (leaf-off and leaf-on), leaf-on C-HH ASAR, leaf-off C-HH ASAR, and leaf-off C-VV ERS data, respectively. These values were selected because they best distinguished wetlands from uplands as observed with field observations, fine-scale aerial photographs, and other supporting data sets (see Section 5.). To create the hydroperiod maps, the first principal component from the PCA was used in an unsupervised ISODATA (Duda & Hart, 1973) classification and resultant classes were later re-grouped and color-coded to better represent variations in PC1 intensity.

PC1 values (a vital input to the binary forested wetlands maps and the only input to the hydroperiod maps) and the binary forested wetland maps were compared with hydrologic data collected at the 24 ground data collection plots; the binary forested wetland and hydroperiod maps were compared with NWI. PC1 values were averaged for the ground data collection plots and regressed against average annual percent area inundated and/or soil moisture for the same plot. Regressions with soil moisture included all plot types while the inundation regressions included only wetland and intermediate plots to

Table 2
Average and standard deviation (SD) percent area inundated, soil moisture (% volumetric water content), tree height, and relative basal area for wetland, intermediate, and upland field plots at the study site

		Inundation	Soil moisture	Tree height	Basal area
		%	(% vwc)	(m)	(m2/ha)
Wetland	Average	26	59	28	38
	SD	7	5	2	3
Intermediate	Average	8	47	28	38
	SD	5	9	2	4
Upland	Average	0	24	26	32
	SD	0	4	1	4

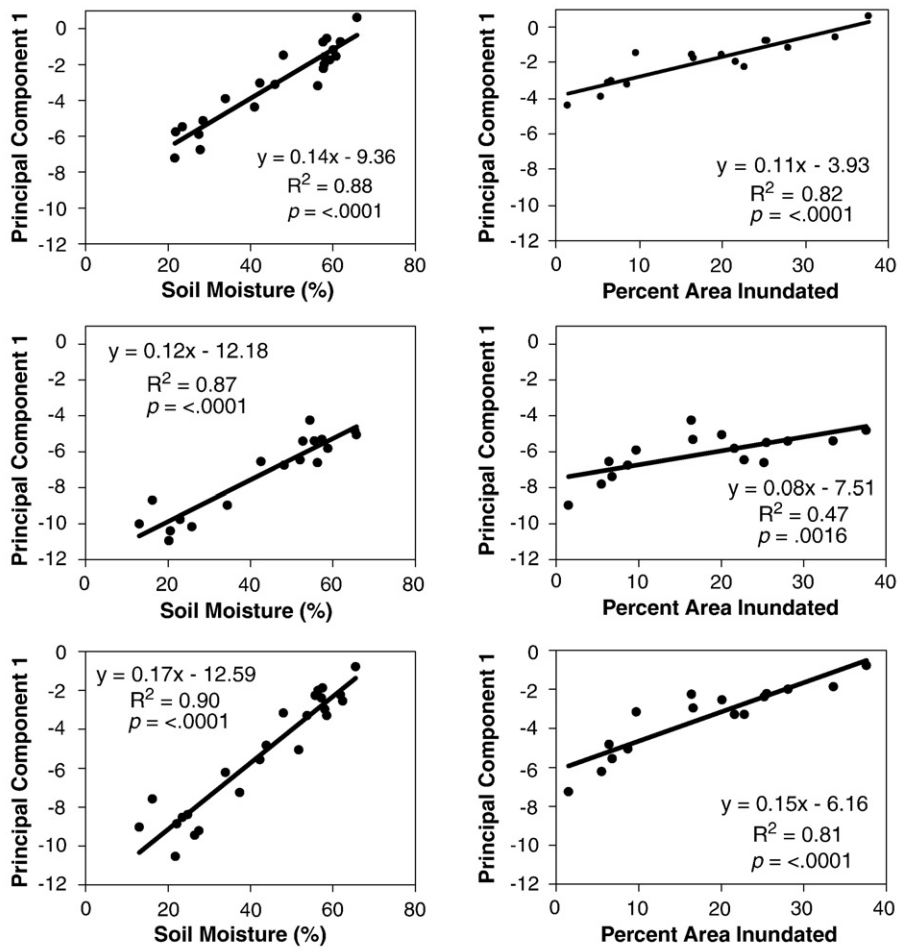

Fig. 3. Regression of percent soil moisture (left column) and percent area inundated (right column) against first principal component of multi-temporal leaf-off ASAR (top), leaf-on ASAR (middle), and C-HH ASAR (bottom). All correlations are significant at the <.0001 level (p=<.0001), except for the correlation between leaf-on ASAR and percent area inundated which is significant at the .0016 level (p=.0016). Soil moisture was considered for all plot types while inundation was only considered for the wetland and intermediate plots to limit the influence of soil moisture. Total uncertainty, including radar fading and absolute calibration errors, in both data sets is 1 dB.

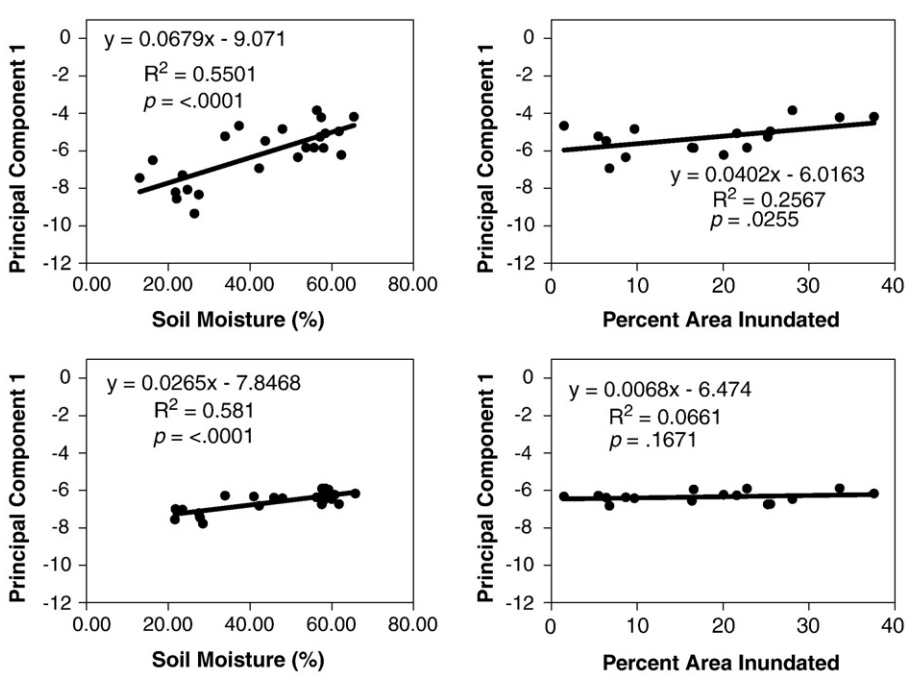

Fig. 4. Regression of percent soil moisture (left column) and percent area inundated (right column) against first principal component of multi-temporal C-VV ASAR (top) and ERS (bottom). Both correlations with soil moisture are significant at the <.0001 level. The correlation between inundation and C-VV ASAR backscatter coefficient is significant at the .0255 level and the correlation between inundation and ERS backscatter coefficient is not significant (p=.1671). Soil moisture was considered for all plot types while inundation was only considered for the wetlands and intermediate plots to limit the influence of soil moisture. Total uncertainty, including radar fading and absolute calibration errors, in both data sets is 1 dB.

Table 3
Validation of binary forested wetland maps at the study site using observations of inundation in field plots

	Wetland areas (25% inundation)				Wetland areas (5% inundation)		
	Correct	Incorrect	Percent		Correct	Incorrect	Percent
Leaf-off ASAR	263	11	95.99	Leaf-off ASAR	771	96	88.93
C-HH ASAR	264	10	96.35	C-HH ASAR	725	142	83.62
C-VV ASAR	173	101	63.14	C-VV ASAR	381	486	43.94
ERS	249	25	90.88	ERS	765	102	88.24
Leaf-on ASAR	239	35	87.23	Leaf-on ASAR	686	181	79.12
	Wetland areas (15% inundation)				Upland areas (false positives)		
	Correct	Incorrect	Percent		Correct	Incorrect	Percent
Leaf-off ASAR	422	21	95.26	Leaf-off ASAR	389	0	100.00
C-HH ASAR	413	30	93.23	C-HH ASAR	389	0	100.00
C-VV ASAR	230	213	51.92	C-VV ASAR	387	2	99.49
ERS	414	29	93.45	ERS	389	0	100.00
Leaf-on ASAR	391	52	88.26	Leaf-on ASAR	389	0	100.00

Correspondence between the binary classification and the plot inundation data is expressed in number of pixels correctly and incorrectly classified and percentage agreement. Comparisons are shown for four thresholds of inundation, 25%, 15%, 5% and 0% of the time. Upland areas with 0% inundation were compared to areas not classified as wetland by the binary maps.

reduce the influence of soil moisture (isolate the relationship with inundation). The areas determined to be forested wetland by the binary SAR classification were compared to areas that were inundated 0%, 5%, 15% and 25% of the time as determined by field observations. The binary forested wetland maps and the hydroperiod maps were visually compared with NWI and a difference matrix was created to more quantitatively compare the binary forested wetland maps with the NWI.

4. Results

Relative basal area within the study plots ranged from 28 to 44 m^2 ha^{-1} (average 35 m^2 ha^{-1}) (Table 2) with upland sites having a slightly lower basal area than the intermediate and wetland sites. Percent visible sky (the complement of canopy closure) varied between 9% during the leaf-on season to 44% during the leaf-off season.

4.1. Validation of PC1 and SAR wetland maps with in situ data

There was a significant (p=<0.05) positive, linear correlation between PC1 values and percent area flooded and soil moisture for all but the correlation between ERS PC1 values and inundation (Figs. 3 and 4). PC1 was found to be more highly correlated with soil moisture (r^2 higher) than with percent area inundated (r^2 lower).

All groups of multi-temporal SAR data used in the binary classification of forested wetlands showed best spatial agreement with the areas that, according to the field data, were flooded on average ≥25% of the time and least with areas flooded for ≤5% of the time (Table 3). Of the five categories of SAR data, the leaf-off C-HH ASAR, the combination of leaf-off and leaf-on C-HH ASAR, and the C-VV ERS classifications had >90% agreement with the field measurements of percent inundation. The C-VV ASAR and the leaf-on ASAR had the lowest agreement.

4.2. Comparison of SAR wetland maps with NWI maps

The difference matrix (Table 4) showed that the leaf-off C-HH ASAR, C-HH ASAR (leaf-off and leaf-on), and ERS (leaf-off, C-VV) compared best, with approximately 90% agreement of wetlands and uplands between the binary classifications and the NWI palustrine forested wetland map. The classifications using the leaf-on ASAR and the C-VV ASAR (leaf-on and leaf-off) data showed 89% and 88% agreement, respectively, with the NWI forested wetland map. In areas that were in disagreement (~5–12% of the total area designated as forested wetland in the NWI), the binary SAR classification was consistently more conservative, identifying a smaller forested wetland area than that demarcated in the NWI. The ASAR C-VV and the leaf-on C-HH ASAR were found to be most conservative.

The majority of the wetlands found in the study area were classified by the NWI as palustrine, forested, broad-leaved, deciduous, and either temporarily flooded (PFO1A) or seasonally flooded (PFO1C). In order to test the ability of SAR to distinguish NWI sub-classes, these sub-divisions were analyzed separately. The sub-class with the longer hydroperiod (PFO1C) was more often identified as forested wetland by the SAR classifications than was the PFO1A class (Table 5).

The binary and hydroperiod maps were visually compared with NWI (Figs. 5 and 6). The binary maps based on C-HH data (Leaf-off ASAR, Leaf-on ASAR, and C-HH ASAR) were found to more accurately distinguish areas with a greater amount of percent inundation than

Table 4
Comparison of the binary Synthetic Aperture Radar (SAR) results with the National Wetlands Inventory (NWI) wetlands map

	PFO1 + (%)	PFO1 − (%)	PFO1C + (%)	PFO1C − (%)	PFO1A + (%)	PFO1A − (%)
C-HH ASAR +	6	2	1	6	4	4
C-HH ASAR −	8	85	1	91	5	87
C-VV ASAR +	3	1	1	3	2	2
C-VV ASAR −	11	85	2	94	7	89
Leaf-off ASAR +	7	3	1	8	5	4
Leaf-off ASAR −	7	84	1	90	5	86
Leaf-on ASAR +	4	2	1	5	3	4
Leaf-on ASAR −	9	84	1	92	6	87
ERS +	6	2	1	7	4	4
ERS −	8	84	1	90	5	87

A difference matrix of percent of total area (rounded to the nearest integer so the totals do not always add up to 100%) between the NWI (top) and the different types of binary SAR maps (left). Marginal labels: ++ indicates positive agreement (they both denote wetland), − indicates negative agreement (they both denote upland), and + — indicates that either the NWI or the classification show wetlands where the other did not. The categories of NWI wetlands used were: All palustrine, broad-leaved deciduous forested (PFO1); palustrine, broad-leaved deciduous forested seasonally flooded (PFO1C); and palustrine, broad-leaved deciduous forested temporarily flooded (PFO1A) wetlands.

Table 5
The increased likelihood that the binary forested wetland maps, created with the radar data sets listed below, identified seasonally flooded in contrast to temporarily flooded areas as indicated by NWI

C-HH ASAR	C-VV ASAR	Leaf-on ASAR	Leaf-off ASAR	ERS
12%	4%	16%	7%	2%

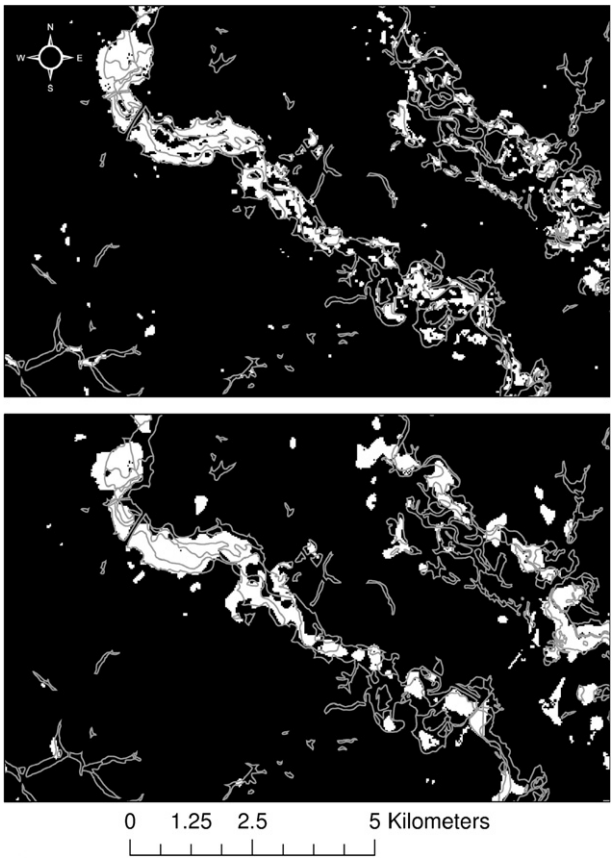

Fig. 5. Binary forested wetland maps created using multi-temporal SAR data (white areas are forested wetland and black areas are not). Top: ASAR C-HH, bottom: ERS C-VV. NWI palustrine forested wetland boundaries are outlined in gray.

those created with C-VV data (ERS and C-VV ASAR), although the maps created with C-VV data still delineated floodplain wetlands (Fig. 5). Areas identified as having longer hydroperiods by the multi-class map followed the NWI boundaries of PFO1C between the seasonally flooded wetlands and the upland edge of the floodplain (Fig. 6). Additionally, the maps follow the subtle borders between the backwater areas (PF01C) and the areas of higher topography surrounding the river (PFO1A).

5. Discussion

Although successful application of C-band data to mapping forested wetlands was initially thought to be unlikely (Hess et al., 1995; Kasischke et al., 1997; Wang et al., 1995), a study by Townsend and Walsh (1998) demonstrated that C-band SAR data could be used to detect areas of ~100% inundation. In this study, we have demonstrated that these data can detect much smaller variations in percent area inundated (<40%), and that they can be used to create maps of forested wetlands and forested wetland hydroperiod. This is in contrast to a recent study by Li and Chen (2005), which had less success using C-band SAR to map forested wetlands using different methods. Bourgeau-Chavez et al. (2001) found that the mapping of forested wetlands using multiple frequency and polarization SAR data was marginal; however, they did not use multi-temporal data, which was found to be an advantage in the present study.

5.1. Utility of optical data for wetland mapping

With both the binary and hydroperiod maps, the use of a forest mask (derived from optical data) was an important first step in mapping forested wetlands. The mask removed land cover types (e.g., residential) characterized by strong backscatter that could be confused with wetlands. With the DEM, anthropogenic increases in backscatter could be further masked and areas where wetlands are unlikely to occur could be removed. The incorporation of visible and infrared imagery in the classification step, however, did not improve the identification of forested wetlands. Although moderate resolution

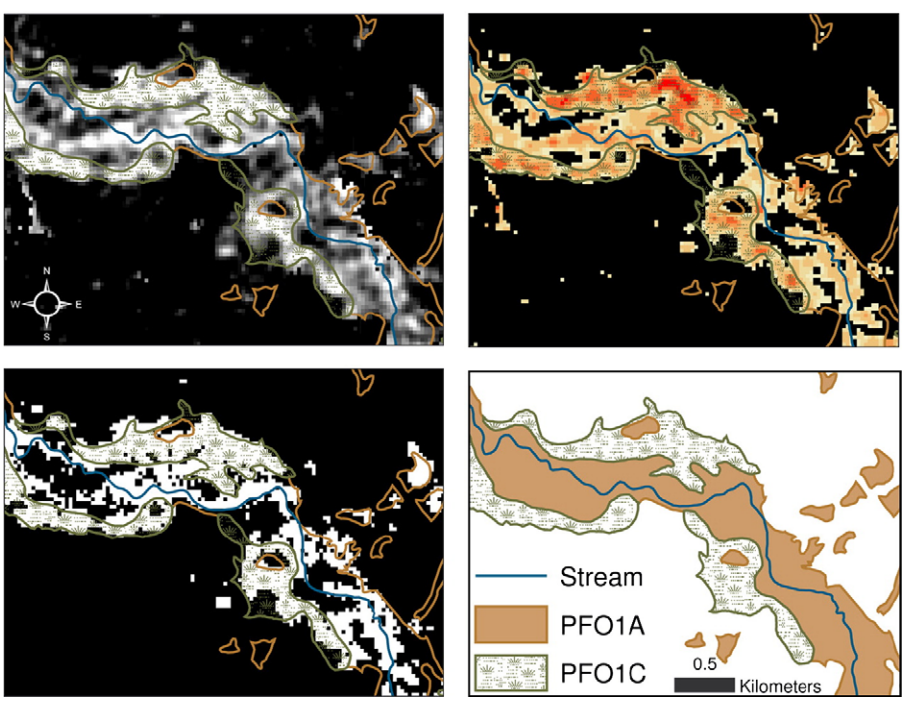

Fig. 6. Multi-temporal ASAR wetland maps. PC1 (top, left), the binary forested wetland map (bottom, left), and the multi-class forested wetland hydroperiod map (top, right) over-laid with the NWI boundaries for palustrine, broad-leaved deciduous, forest with either seasonally (PFO1C — longer flooding duration) or temporarily (PFO1A — shorter duration) flooded wetlands and the boundaries of the Patuxent River. Both types of wetland polygons are shown alone at the bottom right along with the illustration legend. Areas with more flooding and higher amounts of soil moisture through time are displayed in red on the hydroperiod map and those with less flooding and lower levels of soil moisture are displayed in cream.

(~30 m) optical data are well suited for providing information on vegetation type and condition, they are less suited for differentiating subtle differences in hydrology below the forest canopy, especially during the leaf-on season (Carter 1982; Li & Chen, 2005; Moore & North, 1974; Townsend & Walsh, 1998; Toyra & Pietroniro, 2005). In contrast, optical data have been shown to improve the mapping of multiple wetland types, including herbaceous wetlands (Kasischke et al., 1997; Kushwaha et al., 2000; Li & Chen, 2005; Lozano-Garcia & Hoffer, 1993; Toyra et al., 2001, 2002) when used alone or combined with SAR. It is hypothesized that the increased ability of moderate resolution multi-spectral data to map multiple wetland types is primarily due to the ability of optical data to differentiate different vegetation classes. However, this capacity can be partially attributed to the ability of these data to detect large areas of open water through gaps in relatively open vegetative canopies, such as those occurring beneath large expanses of fragmented marsh grass (Rogers & Kearney, 2004). A recent study by Hamilton et al. (2007) used Landsat ETM+ to delineate different types of floodplain vegetation while relying primarily on L-band SAR to locate areas of inundation.

5.2. Validation of PC1 and SAR wetland maps with in situ data

This study supports the work of Townsend (2001) who found that both leaf-on and leaf-off C-HH SAR data were able to accurately detect inundation beneath the forest canopy. As expected, the binary maps of forested wetlands created with C-HH and leaf-off ASAR data agreed the most with *in situ* data (Baghdadi et al., 2001; Hess et al., 1995; Wang et al., 1995). However, the C-VV SAR data and the leaf-on ASAR data performed better than expected based on previous studies (Bourgeau-Chavez et al., 2001; Kasischke et al., 1997; Li & Chen, 2005; Townsend 2002; Townsend & Walsh, 1998; Wang et al., 1995). Again, this may be partially attributable to the multi-temporal approach used in this study. The lower correlation between leaf-on ASAR and inundation observations may be due, in part, to the attenuation and scattering of the microwave energy by the canopy leaves, and in part to a natural reduction in inundation during the times of the year when trees have leaves (increased evapotranspiration). It is important to remember that PC1 values were compared with percent area inundated values averaged throughout the year. Better correlations may be achieved when PC1 values from the multi-temporal leaf-on ASAR are compared with inundation from leaf-on months only.

The fact that PC1 values were better correlated (i.e., higher coefficient of determination) with soil moisture than with inundation was surprising based on previous research (French et al., 1996; Grover et al., 1999). Couturier et al. (2001), however, did find a significant correlation between C-VV backscatter and a weather-based drought index in forested areas. This is consistent with the relationship between C-band backscatter coefficient and soil moisture demonstrated in this study. However it is important to recognize that since hydroperiod incorporates inundation and soil moisture (see Section 1), the relationships between backscatter coefficient and inundation and soil moisture are both vital for the monitoring of wetland extent and functioning. In addition, the correlation between PC1 and hydrologic variables (i.e., inundation and soil moisture) should vary based on site specific conditions. It should be noted that historic ERS C-VV data used in these analyses were acquired in the 1990's, long before the ground-based hydrologic sampling in 2003 and 2004. Correlations with ERS data may therefore be expected to be less strong than those using the ASAR data.

The lower levels of hydroperiod differentiation (i.e., subdividing the floodplain into sections based on time flooded; Fig. 5) using C-VV SAR data may be due to the greater correlation (i.e., higher r^2) of C-VV backscatter with soil moisture and decreased correlation with inundation. Although the levee areas, which are naturally higher than backwater areas, were inundated less (spatially and temporally), these areas often continued to have soil moisture levels that were significantly higher than the surrounding upland areas. While average soil moisture throughout the year in the upland sites was 24%, the wetland sites remained at 59% year round (Table 2), primarily because the water table was closer to the soil surface in the wetlands. Previous studies have also demonstrated positive correlations between microwave backscatter and soil moisture content in non-forested (Kasischke et al., 2003) and forested (Wang et al., 1998) wetlands. Future studies should consider that the influence of soil moisture may be heightened when using C-VV data. The stronger correlation of the leaf-on ASAR data with soil moisture relative to inundation may have been caused by lower levels of inundation present at this time of year (see previous paragraph).

The hydroperiod maps, which were based on multi-temporal SAR data, detected areas that were most likely to be flooded or have saturated soils (high soil moisture). In this way, the hydroperiod maps detected areas that were most likely to exhibit wetland characteristics, such as hydrophytic vegetation and hydric soils (Hamilton et al., 2007; Mitsch & Gosselink, 2000; National Research Council, 1995; Tiner, 1999). Since the varying levels of hydroperiod are not quantitatively defined and the images were not collected at regular intervals throughout the year, these maps depict relative hydroperiod.

5.3. Comparison of SAR wetland maps with NWI maps

The fact that the SAR maps identified a smaller total area of forested wetland as compared to NWI may have partly been caused by real differences in the location and extent of wetlands at the time NWI aerial photographs were acquired and the date of the radar (~25 year difference). However, this is unlikely because the study area was almost entirely within federal lands that are not likely to have been affected by land use change. This is not the case in much of the surrounding area since the Mid-Atlantic is a highly populated and rapidly developing area. Some of the disagreement may be due to inherent limitations of the aerial photographic techniques used in the NWI. Furthermore, the field data collected in this study indicate that the areal extent of forested wetlands may be overestimated by the NWI. For example, the entire floodplain is classified as wetland according to NWI, including areas of higher elevation that do not flood and have relatively low soil moisture. This may be due to the minimum mapping unit of the NWI map or to classification of all floodplain areas as wetland based on potential hydrology due to location (i.e., if an area is in the floodplain it may automatically be labeled as wetland). Therefore, although the comparison of the SAR maps with NWI is a worth-while exercise given that many natural resource managers use NWI data, the field data collected in the study provide the most accurate means of assessment.

5.4. Applicability of presented methods to other regions

A 1999 Forest Inventory and Analysis Program study of Maryland found average basal area to be approximately 23 m^2 ha^{-1} (Forest Inventory and Analysis Program, 1999).Therefore the transmittance of radar energy through an average forest in Maryland would be expected to be greater than or equal to that at the Patuxent study site (Wang et al., 1995).

Although conducted in the Mid-Atlantic U.S., the methods used in this study have widespread potential application. All of the types of data used in this study are or will shortly be available across the U.S. Topographic relief may degrade mapping accuracy, but DEMs can be used to correct for this effect thus increasing the applicability of this technique to a broader region (Kasischke et al., 1997). SAR data are well calibrated, enabling the creation of mosaicked forested wetland maps from images collected over multiple paths and rows. Furthermore, historic C-band SAR data have already been collected for the vast majority of the Mid-Atlantic Coastal Plain and availability of data has increased with the launch of RADARSAT-2. If C-band SAR data are used for regional wetland mapping, the acquisition of a large number of images will necessitate a well-organized effort, as any regional

wetlands mapping program would. However, the simple analysis method described in this paper allows a semi-automated map production approach. This methodology would be substantially less time-consuming than non-automated aerial photograph interpretation, the approach that is currently being used to create the NWI.

As with most environmental phenomena, degree of wetness (i.e., hydroperiod) is continuous in nature, while maps for some management applications must be categorical. The binary map threshold values are not meant to be rigid, predetermined values. This allows for flexibility in the map product. In other words, the inclusiveness of the maps can be adjusted. The user can control whether the product includes a higher or lower degree of wetness, thus increasing the applicability of the method described in this paper to a wider range of projects. The desirable thresholds would, of course, be determined by project goals.

5.5. Future research

The results reported here justify further research on the application of SAR to wetland mapping. Important topics include whether these relative hydroperiod values can be assigned quantitative meaning, such that they can be used in spatially explicit water quality models, such as the Soil and Water Integrated Model (Hattermann et al., 2006). Another critical issue that must be explored before application is whether the technique can be extended to a regional scale. SAR data are available for the entire region and many other areas and so mapping of wooded wetlands is likely to benefit from application of the methods described here. However, expansion of the mapping over significantly larger areas will probably include regions where wetlands will be a much smaller component of the landscape, and it remains to be seen how successful it might be under those conditions. Further studies in the Chesapeake Bay watershed are in progress to test these aspects of the technique.

6. Conclusions

This study demonstrated that C-band SAR data can be used to map deciduous forested wetlands and forested wetland hydroperiod in the Coastal Plain of the Chesapeake Bay Watershed. The techniques and analyses presented in this paper have the potential to support the adaptive management of wetlands and watersheds by: 1) increasing the accuracy of forested wetland maps through the increased sensitivity of SAR to hydrology (i.e., inundation and soil moisture) beneath the forest canopy as compared to optical imagery; 2) decreasing the amount of time and resources necessary to update regional wetland maps via regular acquisition of relatively less expensive (compared to aerial photographs) satellite images and increased speed of digital analysis; and 3) providing temporally appropriate, detailed information on forested wetland hydroperiod that can be used to improve estimates of wetland functioning generally, and the capacity of wetlands to remove pollutants, such as nutrients, specifically. The importance of new methods to rapidly update wetland maps and the need for new tools to assess wetland functions is recognized by the FWS, one of the main federal agencies tasked with monitoring wetlands (U.S. Fish and Wildlife Service, 2002). Although the methods presented in this paper have the potential to improve current wetland mapping approaches, it should be emphasized that this newer technology complements the existing methodology. It does not replace it.

Acknowledgements

This research was conducted while the lead author was a graduate student at the University of Maryland under the supervision of Eric Kasischke. It was supported by a NASA Earth System Science Fellowship and the Mid-Atlantic Regional Earth Science Applications Center. ERS and ENVISAT data were provided by the European Space Agency (ENVISAT AO GRANT 733). The authors would like to thank Robert Adamski, David Asbury, Justin Goldstein, Greg Gude, Khaliah Harmon, Jamison Howard, Jonah Juliano, Binesh Maharjan, Aaron Moss, Josh Slay, Jason Spires, Traci Thompson, Chris Whong, and Nate Workman for assistance in the field. The Vegetation Canopy Lidar group at the University of Maryland graciously loaned their Trimble GPS. Special thanks goes to Holiday Obrecht and the Patuxent Wildlife Research Center for providing access and support for field data collection. The authors gratefully acknowledge the contribution and support of Philip Townsend. The USDA Agricultural Research Service supported the writing and editing of this manuscript. Dr. Martha Anderson reviewed the manuscript and provided many helpful insights. The authors would like to thank the guest editors, Ned Gardiner, Scott Goetz, and Joshua Viers, as well as three anonymous reviewers, for their helpful comments and suggestions.

References

Baghdadi, N., Bernier, M., Gauthier, R., & Neeson, I. (2001). Evaluation of C-band SAR for wetlands mapping. *International Journal of Remote Sensing*, *22*, 71–88.

Boesch, D. F., Brinsfield, R. B., & Magnien, R. E. (2001). Chesapeake Bay eutrophication: scientific understanding, ecosystem restoration, and challenges for agriculture. *Journal of Environmental Quality*, *30*, 303–320.

Bourgeau-Chavez, L. L., Kasischke, E. S., Brunzell, S. M., Mudd, J. P., Smith, K. B., & Frick, A. L. (2001). Analysis of space-borne SAR data for wetland mapping in Virginia riparian ecosystems. *International Journal of Remote Sensing*, *22*, 3665–3687.

Bourgeau-Chavez, L. L., Smith, K. B., Brunzell, S. M., Kasischke, E. S., Romanowicz, E. A., & Richardson, C. J. (2005). Remote sensing of regional inundation patterns and hydroperiod in the greater Everglades using synthetic aperture radar. *Wetlands*, *25*, 176–191.

Carter, V. (1982). Applications of remote sensing to wetlands. In C. J. Johannsen & J. L. Sanders (Eds.), *Remote Sensing for Resource Management (pp. 284–300)* Ankey, Iowa: Soil Conservation Society of America.

Chesapeake Bay Program (1998). *Chesapeake Bay Program land cover, land use, and land practices technical requirements to address Chesapeake Bay agreement policy and restoration goal needs.* Annapolis, Maryland: Chesapeake Bay Program.

Costa, M. P. F. (2004). Use of SAR satellites for mapping zonation of vegetation communities in the Amazon floodplain. *International Journal of Remote Sensing*, *25*, 1817–1835.

Couturier, S., Taylor, D., Siegert, F., Hoffmain, A., & Bao, M. Q. (2001). ERS SAR backscatter: a potential real-time indicator of the proneness of modified rainforests to fire. *Remote Sensing of the Environment*, *76*, 410–417.

Daubenmire, R. F. (1968). *Plant Communities: A Textbook of Plant Synecology.* New York: Harper and Row.

Dobson, M. C., Ulaby, F. T., Pierce, L. E., Sharik, T. L., Bergen, K. M., Kellndorfer, J., Kendra, J. R., Li, E., Lin, Y. C., Nashashibi, A., Sarabandi, K., & Siquei, P. (1995). Estimation of forest biophysical characteristics in northern Michigan with SIR-C/X-S. *IEEE Transactions on Geoscience and Remote Sensing*, *33*, 877–895.

Duda, O., & Hart, P. E. (1973). *Pattern Classification and Scene Analysis.* New York: John Wiley and Sons, Inc.

European Space Agency and Telespazio. (2007). BEST basic Envisat SAR toolbox: User manual, Version 4.0.5, 2007 [Online]. Available from the European Space Agency at http://earth.esa.int/best/ (accessed and verified March 2007).

Federal Geographic Data Committee (1992). *Application of satellite data for mapping and monitoring wetlands — Facts finding report: Technical report 1* Washington, D.C: Wetlands Subcommittee, Federal Geographic Data Committee.

Forest Inventory and Analysis Program. (1999). Forest inventory data [Online]. Available from producer at http://www.fia.fs.fed.us/tools-data/ (accessed March 2005 and verified June 2007).

French, N. H., Kasischke, E. S., Bourgeau-Chavez, L. L., & Harrell, P. A. (1996). Sensitivity of ERS-1 SAR to variations in soil water in fire-disturbed boreal forested ecosystems. *International Journal of Remote Sensing*, *17*, 3037–3053.

Goetz, S. J., Prince, S. D., Thawley, M. M., Smith, A. J., & Wright, R. (2000). The mid-Atlantic Regional Earth Science Applications Center (RESAC): An overview. *ASPRS Annual Conference Proceedings* Washington, D.C.: American Society for Photogrammetry and Remote Sensing (ASPRS).

Grover, K., Quega, S., & Freitas, C. D. (1999). Quantitative estimation of tropical forest cover by SAR. *IEEE Transactions on Geoscience and Remote Sensing*, *37*, 479–490.

Hamilton, S. K., Kellndorfer, J., Lehner, B., & Tobler, M. (2007). Remote sensing of floodplain geomorphology as a surrogate for biodiversity in a tropical river system (Madre de Dios, Peru). *Geomorphology*, *89*, 23–38.

Hattermann, E. F., Krysanova, V., Habeck, A., & Bronstert, A. (2006). Integrating wetlands and riparian zones in river basin modeling. *Ecological Modeling*, *199*, 379–392.

Hess, L. L., Melack, J. M., Filoso, S., & Wang, Y. (1995). Delineation of inundated area and vegetation along the Amazon floodplain with the SIR-C synthetic aperture radar. *IEEE Transactions on Geoscience and Remote Sensing*, *33*, 896–904.

Hess, L. L., Melack, J. M., & Simonett, D. S. (1990). Radar detection of flooding beneath the forest canopy: A review. *International Journal of Remote Sensing*, *11*, 1313–1325.

Kasischke, E. S., Melack, J. M., & Dobson, M. C. (1997). The use of imaging radars for ecological applications — A review. *Remote Sensing of Environment*, *59*, 141–156.

Kasischke, E. S., Smith, K. B., Bourgeau-Chavez, L. L., Romanowicz, E. A., Brunzell, S., & Richardson, C. J. (2003). Effects of seasonal hydrologic patterns in south Florida wetlands on radar backscatter measured from ERS-2 SAR imagery. *Remote Sensing of Environment*, *88*, 423–441.

Kauth, R. J., & Thomas, G. (1976). The tasselled cap — A graphic description of the spectral–temporal development of agricultural crops as seen by Landsat. *Symposium on Machine Processing on Remotely-Sensed Data* West Lafeyette, IN: Purdue University.

Koeln, G., & Bissonnette, J. (1999). *Cross-correlation analysis: Mapping land cover changes with a historic land cover database and a recent, single-date, multispectral image.* Rockville, M.D.: Earth Satellite Corporation.

Korb, J. E., Covington, W. W., & Fule, P. Z. (2003). Sampling techniques influence understory plant trajectories after restoration: An example from ponderosa pine restoration. *Restoration Ecology*, *11*, 504–515.

Kudray, G. M., & Gale, M. R. (2000). Evaluation of National Wetland Inventory maps in a heavily forested region in the upper Great Lakes. *Wetlands*, *20*, 581–687.

Kushwaha, S. P. S., Dwivedi, R. S., & Rao, B. R. M. (2000). Evaluation of various digital image processing techniques for detection of coastal wetlands using ERS-1 SAR data. *International Journal of Remote Sensing*, *21*, 565–579.

Li, J., & Chen, W. (2005). A rule-based method for mapping Canada's wetlands using optical, radar and DEM data. *International Journal of Remote Sensing*, *26*, 5051–5069.

Lozano-Garcia, D. F., & Hoffer, R. M. (1993). Synergistic effects of combined Landsat-TM and SIR-B data for forest resources assessment. *International Journal of Remote Sensing*, *14*, 2677–2694.

Lunetta, R. S., & Balogh, M. E. (1999). Application of multi-temporal Landsat 5 TM imagery for wetland identification. *Photogrammetric Engineering and Remote Sensing*, *65*, 1303–1310.

Mid-Atlantic Regional Assessment Team (2000). *Preparing for a changing climate: The potential consequences of climate variability and change: U.S. Environmental Protection Agency and Pennsylvania State University.*

Mitsch, W. J., & Gosselink, J. G. (2000). *Wetlands.* New York: John Wiley & Sons, Inc.

Moore, G. K., & North, G. W. (1974). Flood inundation in the southeastern United Sates from aircraft and satellite imagery. *Water Resources Bulletin*, *10*, 1082–1096.

Moore, M. V., Pace, M. L., Mather, J. R., Murdoch, P. S., Howarth, R. W., Chen, C. Y., Flebbe, P. A., Folt, C. L., Hemond, H. F., & Driscoll, C. T. (1997). Potential effects of climate change on freshwater ecosystems of the New England/mid-Atlantic region. *Hydrological Processes*, *11*, 925–947.

Morrissey, L. A., Livingston, G. P., & Durden, S. L. (1994). Use of SAR in regional methane exchange studies. *International Journal of Remote Sensing*, *15*, 1337–1342.

National Research Council (1995). *Wetlands: Characteristics and Boundaries.* Washington: National Academy Press.

Neusch, T., & Sties, M. (1999). Application of the Dubois-model using experimental synthetic aperture radar data for the determination of soil moisture and surface roughness. *ISPRS Journal of Photogrammetry and Remote Sensing*, *54*, 273–278.

Nichols, C. (1994). *Map accuracy of National Wetlands Inventory maps for areas subject to land use regulation commission jurisdiction.* Hadley, MA: U.S. Fish & Wildlife Service, Northeast Region.

Richards, J. A., Woodgate, P. W., & Skidmore, A. K. (1987). An explanation of enhanced radar backscatter from flooded forests. *International Journal of Remote Sensing*, *8*, 1093–1100.

Rogers, A. S., & Kearney, M. S. (2004). Reducing signature variability in unmixing coastal march Thematic Mapper scenes using spectral indices. *International Journal of Remote Sensing*, *25*, 2317–2335.

Rolband, M. S. (1995). A comparison of wetland areas in northern Virginia: National wetland inventory maps versus field delineated wetlands under the 1987 manual. *Wetland Journal: Research, Restoration, Education*, *7*, 10–14.

Rosich, B. & Meadows, P. (2004). Absolute calibration of ASAR level 1 products generated with PF-ASAR, Version 1.5, 2004 [Online]. Available from the European Space Agency at http://envisat.esa.int/object/doc.cfm?fobjectid=4503 (accessed and verified June 2007).

Rulequest Research. (2004). Data mining tools See5 and C5.0 [Online]. Available from Rulequest Research at http://www.rulequest.com/see5-info.html (posted November 2004; verified March 2007).

Sader, S., Ahl, D., & Liou, W. (1995). Accuracy of Landsat-TM and GIS rule-based methods for forest wetland classification in Maine. *Remote Sensing of Environment*, *53*, 133–144.

Shiver, B., & Borders, B. (1996). *Sampling Techniques for Forest Resource Inventory.* New York: John Wiley & Sons, Inc.

Stolt, M. H., & Baker, J. C. (1995). Evaluation of National Wetland Inventory maps to inventory wetlands in the southern Blue Ridge of Virginia. *Wetlands*, *15*, 346–353.

Tiner, R. (1987). *Mid-Atlantic wetlands — A disappearing natural treasure.* Hadley, MA: U.S. Fish & Wildlife Service, Ecological Services, Northeast Region.

Tiner, R. (1990). Use of high altitude aerial photography for inventorying forested wetlands in the United States. Forest Ecology and Management, 33–34, 593–604.

Tiner, R. (1999). *Wetland Indicators: A Guide to Wetland Identification, Delineation, Classification, and Mapping.* Washington: Lewis Publishers.

Townsend, P. A. (2000). A quantitative fuzzy approach to assess mapped vegetation classifications for ecological applications. *Remote Sensing of Environment*, *72*, 253–267.

Townsend, P. A. (2001). Mapping seasonal flooding in forested wetlands using multi-temporal Radarsat SAR. *Photogrammetric Engineering and Remote Sensing*, *67*, 857–864.

Townsend, P. A. (2002). Relationships between forest structure and the detection of flood inundation in forested wetlands using C-band SAR. *International Journal of Remote Sensing*, *23*, 443–460.

Townsend, P. A., & Walsh, S. J. (1998). Modeling floodplain inundation using an integrated GIS with radar and optical remote sensing. *Geomorphology*, *21*, 295–312.

Toyra, J., & Pietroniro, A. (2005). Towards operational monitoring of a northern wetland using geomatics-based techniques. *Remote Sensing of Environment*, *97*, 174–191.

Toyra, J., Pietroniro, A., & Martz, L. W. (2001). Multisensor hydrologic assessment of a freshwater wetland. *Remote Sensing of Environment*, *75*, 162–173.

Toyra, J., Pietroniro, A., Martz, L. W., & Prowse, T. D. (2002). A multi-sensor approach to wetland flood monitoring. *Hydrological Processes*, *16*, 1569–1581.

U.S. Fish & Wildlife Service (2002). National Wetlands Inventory: A strategy for the 21st century [Online]. Available from Department of the Interior http://www.nwi.fws.gov/Pubs_Reports/NWI121StatFNL.pdf (posted January 2002; verified March 2007).

U.S. Geological Survey (2004). National elevation dataset 1/3 arc second [Online]. Available from U.S. Geological Survey at http://seamless.usgs.gov (Accessed: October 28, 2004; verified March 2007).

Varlyguin, D., Wright, R., Goetz, S. J., & Prince, S. D. (2001). Advances in land cover classification for applications research: A case study from the mid-Atlantic RESAC. *American Society for Photogrammetry and Remote Sensing (ASPRS) Conference Proceedings, St. Louis, MO*.

Vieglais, D. A., & Rich, P. M. (1997). *HemiView analysis of hemispherical imagery.* Delta-T Devices Ltd.

Wang, Y., Day, J. L., & Davis, F. W. (1998). Sensitivity of modeled C- and L-band radar backscatter to ground surface parameters in loblolly pine forest. *Remote Sensing of Environment*, *66*, 331–342.

Wang, Y., Hess, L. L., Filoso, S., & Melack, J. M. (1995). Understanding the radar backscattering from flooded and non-flooded Amazonian forests: Results from canopy backscatter modeling. *Remote Sensing of Environment*, *54*, 324–332.